

Received June 5, 2017, accepted June 15, 2017, date of publication June 19, 2017, date of current version July 7, 2017.

Digital Object Identifier 10.1109/ACCESS.2017.2717493

# MAS-Based Hierarchical Distributed Coordinate Control Strategy of Virtual Power Source Voltage in Low-Voltage Microgrid

CHUNXIA DOU<sup>1,2</sup>, ZHANQIANG ZHANG<sup>1</sup>, DONG YUE<sup>2</sup>, (Senior Member, IEEE),  
AND YUHANG ZHENG<sup>1</sup>

<sup>1</sup>Institute of Electrical Engineering, Yanshan University, Qinhuangdao 066004, China

<sup>2</sup>Institute of Advanced Technology, Nanjing University of Posts and Telecommunications, Nanjing 210023, China

Corresponding author: Chunxia Dou (cxdou@ysu.edu.cn)

This work was supported in part by the National Natural Science Foundation of China under Grant 61573300, and Grant 61533010 and in part by the Hebei Provincial Natural Science Foundation of China under Grant E2016203374.

**ABSTRACT** To settle reactive power sharing inaccuracy among distributed generations (DGs) associated with mismatched lines impedance, a hierarchical control strategy in the framework of multi-agent system (MAS) is proposed. Replace DG by virtual power source (VPS) in droop control and synchronize VPSs voltages by a hierarchical control. Initially, in primary control, improve line feature by defining virtual impedance value, so that VPSs voltages are roughly consistent. Then, design a VPS voltage evaluation index based on reactive power outputs, whose trigger determines whether secondary control is activated. Finally, in secondary control, consensus protocol is used to strictly synchronize actual VPSs voltages with limited voltages information exchange by the sparse communication network. Therefore, MAS is used to provide an appropriate DGs interaction manner and hierarchical control frame. Each DG is associated with a first-level distributed agent to execute primary control. Coordination part is regarded as secondary-level agents to realize secondary control. Hierarchical control provides double safeguards of VPSs voltages synchronization. To verify the effects of control strategy, simulations are carried out on RTLAB and MATLAB/Simulink.

**INDEX TERMS** Reactive power sharing, virtual power sources (VPSs), VPS voltage evaluation index (VVEI), consensus protocol, multi-agent system (MAS).

## I. INTRODUCTION

Microgrid comprised of the distributed generations (DGs), energy storage systems, loads and its control system, has been proposed to integrate various renewable sources, such as wind turbine, photo-voltaic, micro-turbines and storage battery in the forms of DGs [1]–[3]. Generally, microgrid can operate on both grid-connected mode and islanded mode. Microgrid will disconnect from grid and switch to islanded mode under some disturbances [4]. In islanded microgrid, an appropriate control method is necessary to guarantee that the microgrid operation is stable, e.g. coordinate the dispatched active and reactive powers of all the DGs based on their capacities.

Droop control method implementing DGs' plug-and-play function and peer-to-peer control, is suitable for islanded mode. The control objective is to regulate DGs voltage amplitude as well as running frequency by supplying necessary DGs reactive power and active power outputs. Generally, DGs in a microgrid share the total powers demands of

loads based on their respective maximum generation capabilities or inverse ratio of droop coefficients. When multiple DGs supply public loads, reactive power sharing accuracy is discounted greatly for the discrepant DGs voltages amplitudes. Ultimately, it attributes to the mismatching in non-negligible lines impedance [5]–[7]. Especially in low-voltage microgrid, power coupling is also associated with mainly resistive line impedance [8]. Hence, measures are extremely necessary to improve powers performance.

To maintain microgrid powers balance, a hierarchical control, including primary and secondary control, can be conventionally used to control DGs [9], [10]. Droop control as a primary control is used to locally regulate individual DG voltage in a distributed way. Secondary control coordinating all the DGs voltages by a necessary communication network is realized in a centralized way. Inspired by a coordinate control in multi-agent systems (MAS) [11]–[13], each DG agent in the microgrid is associated with a first-level agent which

exchanges information with their neighbor agents according to some communication protocols in an upper secondary-level agent [14]. The coordination protocol as secondary control can make decisions that first-level agents must execute by analyzing exchanged information. Global state synchronization of each agent is the main control objective of MAS. State variables coordination of each agent determines the efficiency of hierarchical control.

Paper [15] proposes a centralized hierarchical control to eliminate the voltages and frequencies deviation, but complex communication link among local controller of DGs and central controllers are required. Besides, when communication link is interrupted, entire control can lose efficacy. An autonomous powers control strategy implements powers management in a decentralized way in [16], [17]. Primary control realizes powers management function and secondary control strictly regulates voltage and frequency to compensate powers deviations, which relies on high speed communication. A local voltage regulation method without communication is proposed in [18]. But it is limited to single DG and inadaptable for multiple DGs. In order to realize desired power sharing without communication among DGs, reactive power sharing deviation is estimated by injecting a small power disturbance in [19]. The control is realized by the low-bandwidth signals from central controller. MAS-based secondary voltage cooperative control is proposed in [20], [21]. Consensus theory is used to synchronize global DGs voltages via the sparse communication networks. Paper [22] proposes a voltage compensation method using dynamic consensus algorithm. Performance in reactive power sharing is well. Dynamic consensus algorithm is used popularly in MAS [23], [24].

For a microgrid with mismatched lines impedance, it is hard to eliminate the differences in DGs voltages, but it is easily realized if use virtual power sources (VPSs) to cooperate with virtual impedance in this paper. More precisely, when virtual impedance is firstly used to change lines feature, VPSs voltages can be then synchronous. To obtain the accurate reactive power sharing, MAS-based hierarchical distributed coordinate control strategy of VPS voltage instead of DG voltage is proposed. The innovative works of proposed control strategy are as follows.

(i) In primary control, replace DG by VPS, realized through improving parameters of droop controller and proposing virtual controller that is used to realize the virtual impedance. Primary control of VPSs voltages synchronization is realized locally by choosing value of virtual impedance.

(ii) Secondary control coordinates actual VPSs voltages by consensus protocol so as to strictly synchronize VPSs voltages. Due to the actually nonexistent VPS in networks, actual VPSs voltages are compounded by actual DGs voltages and voltages drops in virtual impedance.

(iii) Cooperation between primary and secondary controls is based on the established VPS voltage evaluation index (VVEI). Its design is based on DGs reactive power outputs.

If any one of actual VPSs voltages triggers VVEI, secondary control will be activated immediately.

(iv) Both primary and secondary controls can independently regulate VPSs voltages. Thus, it provides double safeguards in synchronizing VPSs voltages. The difference is reflected in the control precision.

This paper is organized as follows. Section II gives the MAS-based hierarchical control strategy. Section III gives the proposed hierarchical distributed coordinate control strategy of VPSs voltages, including designs of primary controller, VVEI and secondary controller. Section IV gives the simulation results. Section V summarizes the paper and gives the conclusion.

## II. MAS-BASED MICROGRID HIERARCHICAL CONTROL FRAME

The MAS as a distributed autonomous computational system is constituted by multiple agents, and MAS is also a branch of the tendency of artificial intelligence technology [12], [25]. MAS can coordinate and control all the agents, combining with their autonomic behavior and the negotiation between agents, so that optimize the agents performance. Meanwhile, MAS relying on the improvement of intelligence levels provides a unified frame for some actual systems and settles the communication problem of complex systems. MAS-based control strategy for microgrid can provide an appropriate information interaction manner and hierarchical control frame in coordinating and controlling DGs.

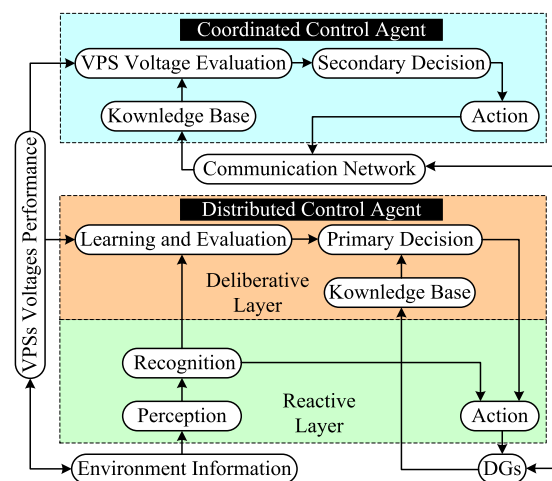


FIGURE 1. Structure of hierarchical distributed coordinate control based on MAS.

Microgrid is a typical distributed system where MAS can strengthen the coordinate control between DG and DG or DG and load. In hierarchical distributed coordinate control of microgrid, first-level distributed agents including DG agents and load agents are used to realize the local primary control for DGs. Each first-level agent is designed as a hybrid agent containing reactive layer and deliberative layer, shown in Fig. 1. Reactive layer composed of perception, recognition and action models can respond preferentially and act

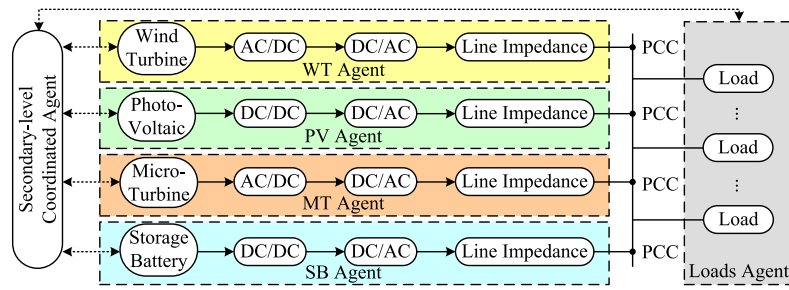


FIGURE 2. MAS-based structure of microgrid.

quickly in emergency [26]. Deliberative layer composed of belief, desire and intent models has high intelligence in optimizing the behavior of DGs agents. Primary controllers, mainly including droop controller, virtual controller and voltage/current controller, can roughly synchronize VPSs voltages.

The secondary-level coordinated agent has a higher level of deliberative layer in Fig. 1, whose start depends on VPS voltage evaluation model. It is mainly responsible for strictly synchronizing VPSs voltages by information exchanges of DG agents via the sparse communication network. VPS voltage evaluation model evaluates the deviation size of actual VPS voltage based on its performance and decides whether the secondary control starts in decision model. Actual VPS voltage as the secondary control input comes from primary control. Secondary control output sends command to virtual controller of primary control by the action module. Secondary controllers, mainly including consensus controller and involving partial switch controller, are used to realize the strict accuracy control of VPSs voltages.

Generally, the interactive manner of agents includes master-slave manner among different levels of agents and peer-peer manner among same level of agents. In the master-slave manner, first-level agent must execute the command from secondary-level agent. In the peer-peer manner, same level of agents should equally exchange mutual information. An islanded microgrid including various DGs (e.g. wind turbine, photo-voltaic, micro-turbine and storage battery, etc) is shown in Fig. 2, where each DG as a first-level distributed agent connects to public loads agent across line impedance. In this paper, the discussed DGs are the same type, so the control scheme of all inverters is consistent. Via the sparse communication network, all the DG agents can exchange mutual VPS voltages information and loads agent uploads their powers command information. Then, secondary-level coordinated agents address above information and respond immediately to DG agents.

### III. HIERARCHICAL DISTRIBUTED COORDINATE CONTROL STRATEGY OF VPS VOLTAGE

This section describes the control strategy of VPS voltage. In distributed primary control, improve droop feature of VPS by

defining value of virtual impedance, so that VPSs voltages are roughly synchronized. In coordinated secondary control, consensus protocol is used to strictly synchronize VPSs voltages. Besides the above two levels controls, there is a switch control, where VVEI is designed by series of DGs reactive power outputs. When deviation of actual VPS voltage in primary control triggers VVEI in certain cases, secondary control will be activated.

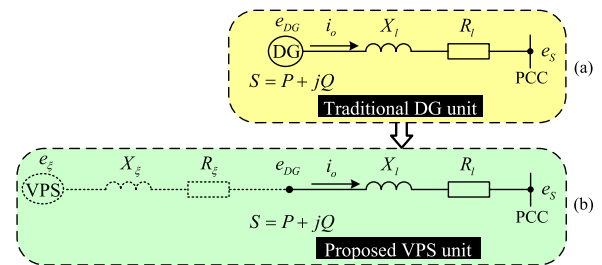


FIGURE 3. Equivalent circuits of DG unit and VPS unit.

#### A. VPS VOLTAGE PRIMARY CONTROL BASED ON VIRTUAL IMPEDANCE

The mainly line resistance in low-voltage microgrid easily leads to power coupling and reactive power sharing inaccuracy. This paper proposes a control method combining VPS control with virtual impedance. Based on line impedance feature improved by virtual impedance, the VPSs voltages synchronization decides DGs reactive power sharing accuracy. Equivalent circuits of DG and VPS units are illustrated in Fig. 3, where  $e_\xi$  is the VPS voltage,  $R_\xi$  is the virtual resistance,  $X_\xi$  is the virtual inductance,  $S$  is the DG powers output,  $R_l$  is the line resistance and  $X_l$  is the line inductance. For constructing an inductive power decoupling environment, virtual resistance is equal to negative line resistance ( $R_\xi = -R_l$ ), and select virtual inductance by (7). The droop equation about controlling VPS voltage based on DG powers output is given by

$$f_\xi = f_\xi^* - m_\xi(P^* - P) \tag{1}$$

$$E_\xi = E_\xi^* - n_\xi(Q^* - Q) \tag{2}$$

where  $m_\xi, n_\xi$  are the droop coefficients expressed as

$$m_\xi = (f_\xi^* - f_{\xi-\min}) / (P^* - P_{\max}) \quad (3)$$

$$n_\xi = (E_\xi^* - E_{\xi-\min}) / (Q^* - Q_{\max}) \quad (4)$$

where  $P^*/Q^*$  is the active/reactive power reference of DG,  $P_{\max}/Q_{\max}$  is the maximum active/reactive power capacity of DG,  $f_\xi^*/E_\xi^*$  is the frequency/voltage reference of VPS, and  $f_{\xi-\min}/E_{\xi-\min}$  is the minimum allowable frequency/voltage of VPS. Generally, DGs need to have the same running frequencies for satisfying global frequency consistency, which makes the same frequency control algorithm to be used for DGs, so that active power sharing is accurate [7]. For virtual impedance hardly affects system frequency, VPS frequency is the same as DG. So in terms of VPS voltage control, amplitude differences are harmful to VPSs voltages synchronization. So some important parameters affecting VPS voltage amplitude are contained in equations (5) and (6)

$$\begin{aligned} E_\xi^* &= E^* + E_v^* + E_l^* \\ &= E^* + (X_\xi Q^* + R_\xi P_{Q^*}) / E^* + (X_l Q^* + R_l P_{Q^*}) / E^* \\ &= E^* + [(X_\xi + X_l) Q^*] / E^* \end{aligned} \quad (5)$$

$$\begin{aligned} E_{\xi-\min} &= E_{v-Q_{\max}} + E_{l-Q_{\max}} + E_{\min} \\ &= \frac{X_\xi Q_{\max} + R_\xi P_{Q_{\max}}}{E^*} + \frac{X_l Q_{\max} + R_l P_{Q_{\max}}}{E^*} + E_{\min} \\ &= E_{\min} + \frac{(X_\xi + X_l) Q_{\max}}{E^*} \end{aligned} \quad (6)$$

where  $E_v^*/E_{v-Q_{\max}}$  is the virtual voltage drop,  $E_l^*/E_{l-Q_{\max}}$  is the line voltage drop, and  $P_{Q^*}/P_{Q_{\max}}$  is the DG active power output when DG dispatch reference/maximum reactive power.

Reactive power sharing inaccuracy is inevitable for the DGs voltages differences caused by mismatched lines impedance. Meanwhile, DGs voltages synchronization control and circulation current control are mutually conditioned (i.e. when lines currents are equal, DGs voltages will be discrepant for unequal lines voltages drops; when DGs voltages are consistent, lines currents will be discrepant for unequal lines impedance). So improve the line impedance features through defining values of DGs virtual inductance:

$$\frac{X_{\xi m} + X_{lm}}{X_{\xi n} + X_{ln}} = \frac{n_{\xi m}}{n_{\xi n}} \quad (7)$$

*Proof:* In (2), to realize accurate reactive power sharing between DGm and DGn ( $Q_m/Q_n = n_{\xi n}/n_{\xi m}$ ), VPSs voltages should be equal ( $E_{\xi m} = E_{\xi n}$ ). In Fig. 3(b), the voltages drop in  $X_{\xi m} + X_{lm}$  and  $X_{\xi n} + X_{ln}$  need to be equal:

$$\frac{(X_{\xi m} + X_{lm})Q_m}{E^*} = \frac{(X_{\xi n} + X_{ln})Q_n}{E^*} \quad (8)$$

If we want to obtain  $Q_m/Q_n = n_{\xi n}/n_{\xi m}$  in (8), we need to define the values of virtual inductance as (7).

Thus, based on (7), VPSs voltages synchronization primary control instead of DGs may be realized. To avoid the harmonics increasing, virtual negative inductance is proposed [27] under the premise of satisfying (7). Only in this condition

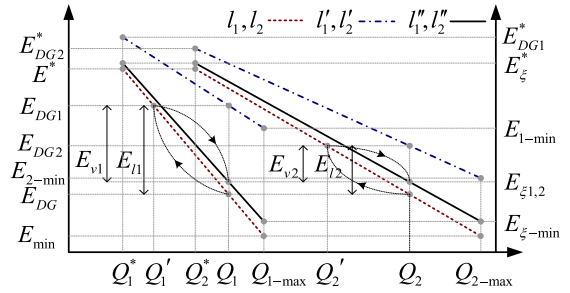


FIGURE 4. Droop features of DG and VPS with considering voltages drops in lines impedance and virtual impedance.

as (7), VPSs voltages references and minimum allowable voltages in (5) and (6) will be consistent.

In Fig. 4, lines  $l_1, l_2$  represent the traditional droop lines of DGs (DG1, DG2) without considering any voltage drop, lines  $l'_1, l'_2$  represent the actual droop lines considering lines voltages drops, lines  $l''_1, l''_2$  represent the droop lines of VPSs (VPS1, VPS2) considering lines and virtual voltage drops. When lines  $l_1, l_2$  are used for reactive power control, the actual sharing as  $Q'_1 : Q'_2$  deviates from ideal sharing as  $Q_1 : Q_2$  due to different actual DGs voltages ( $E_{DG1}, E_{DG2}$ ) caused by the unequal lines voltages drops ( $E_{l1}, E_{l2}$ ). In terms of lines  $l''_1, l''_2$ , intervention of virtual voltages drops ( $E_{v1}, E_{v2}$ ) narrows the deviation with lines  $l_1, l_2$ , relative to lines  $l'_1, l'_2$ . This is due to the relatively consistent VPSs voltages amplitudes in (8). Under the effect of voltage drops in line and virtual impedance, each point in lines  $l''_1, l''_2$  is derived from corresponding point in lines  $l_1, l_2$ . When lines  $l'_1, l'_2$  are used to reactive power sharing, accuracy will be restored to desired value. Although the lines  $l'_1, l'_2$  adaptable to actual DGs voltages are also used to realize accurate sharing, the signal deviation of DGs voltages in secondary control may be unsuitable for consensus protocol. And the effect of VPSs voltage synchronization in secondary control may be reduced. Hence, (7)-based droop equation (2) is regarded as the primary control so as to roughly synchronize VPSs voltages.

Designs of primary controllers, including droop controller, virtual controller and voltage/current controller, are given in Fig. 5. As explained early, droop controller is used to simulate VPS and realize VPS voltage primary control cooperating with virtual controller where virtual impedance can be realized by subtracting virtual voltage drop from VPS voltage  $e_\xi$ :

$$\begin{cases} v_{od}^* = e_{\xi d} - e_{vd} \\ v_{oq}^* = e_{\xi q} - e_{vq} \end{cases} \quad (9)$$

where  $v_{od}^*, v_{oq}^*$  are the instruction voltages of voltage/current controller in the dq frame,  $e_{vd}, e_{vq}$  are the virtual voltage drops in the dq frame, expressed as

$$\begin{cases} e_{vd} = R_\xi i_{od} - \omega L_\xi i_{oq} \\ e_{vq} = R_\xi i_{oq} + \omega L_\xi i_{od} \end{cases} \quad (10)$$



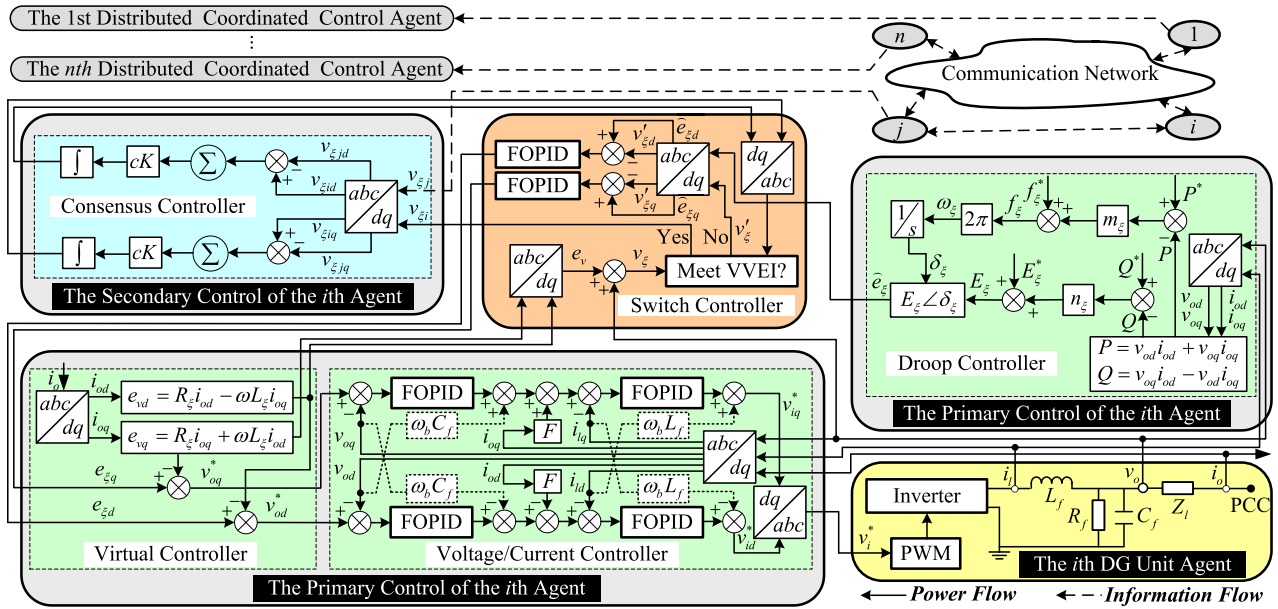


FIGURE 5. Implementation of the proposed hierarchical distributed coordinate control of VPSs voltages.

FOPID-based (fractional-order PID) voltage/current controller is used to control inverter voltage tracking the afore-said instruction voltage in (9). The increase in two freedom degrees of order makes controller flexible. For obtaining the desired modulation signal, FOPID controller parameters are optimized by differential evolution algorithm [28].

However, primary control of VPSs voltages may not strictly synchronize VPSs voltages in some situations (e.g. large loads demands). Thus, actual VPSs voltages will satisfy VVEI, and then consensus controller is instantly executed to strictly improve the synchronization precision.

**B. THE VVEI DESIGN**

VPS voltage evaluation in secondary-level agent determines whether secondary control of VPSs is activated. A reliable and appropriate VVEI is designed in this section. The voltage participating in evaluation is selected as actual VPS voltage compounded by actual DG voltage and virtual voltage drop from virtual controller. Based on DGs reactive power outputs, VVEI is designed.

Actual reactive power output of each DG can be obtained from power calculation mode in respective droop controller. Desired reactive power output of each DG is based on the total loads power demand and sharing proportion. Vectors of actual and desired DGs reactive power outputs can be assumed as  $\mathbf{Q} = [Q_1, Q_2, \dots, Q_N]^T$  and  $\hat{\mathbf{Q}} = [\hat{Q}_1, \hat{Q}_2, \dots, \hat{Q}_N]^T$ , where

$$\hat{Q}_i = k_i Q_l = \left[ (1/n_{\xi i}) / \sum_{j=1}^N \frac{1}{n_{\xi j}} \right] Q_l \quad (11)$$

where  $Q_l$  is the total loads reactive power demands,  $k_i$  is the sharing proportion coefficient of  $i$ th DG. It is easy to derive as

$\sum_{i=1}^N k_i = 1$ , which indicates the total loads power demand can be completely supplied by all the DGs.

*Definition 1:* The sharing deviation is unallowable when actual reactive power of  $i$ th DG deviates more than  $c\%$  (include  $c\%$ ) of its maximum reactive power capacity from desired value:

$$|Q_i - \hat{Q}_i| \geq c\% Q_{imax} \quad (12)$$

The dispatched reactive power output of each DG can't exceed maximum capacity or be less than reference value, which is associated with evaluation of  $c\%$ . Besides, value of  $c\%$  depends on the required precision. So value of  $c\%$  should be as small as possible. Based on (2), (11) and (12), the unallowable deviation of  $i$ th VPS voltage (i.e. VVEI) is expressed as

$$V_{\xi i} \geq / \leq E_{\xi}^* + \left( 1 / \sum_{j=1}^N \frac{1}{n_{\xi j}} \right) Q_l - / + n_{\xi i} c\% Q_{imax} \quad (13)$$

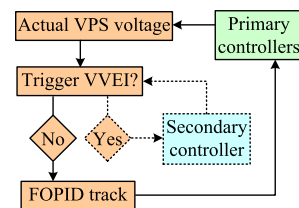


FIGURE 6. Cooperation between primary control and secondary control.

The relevant controller is switch controller in Fig. 5, which contributes to the cooperation of primary and secondary controllers. Detailed cooperation principle is described

in Fig. 6, where switch of primary control and secondary control relies on whether actual VPS voltage triggers VVEI. The actual VPS voltage  $v_\xi$  is synthesized firstly in switch controller by certain variables from primary controllers. Then, consensus controller of  $i$ th DG agent, which cooperates with the primary controllers to synchronize VPS voltage, is activated if its actual VPS voltage triggers VVEI. FOPID whose principle in switch controller is similar to voltage/current controller can be used to control the allowable actual VPS voltage  $v'_\xi$  tracking the VPS voltage instruction  $\hat{e}_\xi$  from primary controllers. VPS voltage outputted from consensus controller also requires evaluation. Then, VPS voltage can be used directly to FOPID track once the VVEI is not triggered, otherwise, continue to activate secondary control.

**C. VPS VOLTAGE SECONDARY CONTROL BASED ON CONSENSUS CONTROL THEORY**

Consensus control theory has been used widely in various fields especially in microgrid [29], [31]. The objective of consensus control is achieving states synchronization of agents in global system by a communication network. It can be used to coordinate multiple DGs in the framework of MAS through limited information exchange. In consensus controller, consensus control theory is used to realize the secondary control. Thus, strictly accurate reactive sharing is realized by strictly consistent VPSs voltages. Namely, when rough synchronization in primary control is unallowable, secondary control will strictly synchronize VPSs voltages. And primary control also has ability to roughly regulate in return if the communication link fails.

A microgrid can be considered as the MAS, where each DG is an agent [30]. The VPS voltage secondary control is established by using consensus protocol to deal with the interacted information of DGs agents via sparse communication network. The communication network link can be modeled by a digraph  $G_d(\mathbf{V}_G, \mathbf{E}_G, \mathbf{A}_G)$  with a finite node set  $\mathbf{V}_G = \{V_1, V_2, \dots, V_N\}$ , a communication link set  $\mathbf{E}_G \subseteq \mathbf{V}_G \times \mathbf{V}_G$  and an adjacency matrix  $\mathbf{A}_G = [a_{ij}]_{N \times N}$ . An edge from node  $j$  to node  $i$  is expressed as  $(V_j, V_i)$ , which means that node  $i$  receives information from node  $j$ . Node  $i$  is called a neighbor of node  $j$  if  $(V_j, V_i) \in \mathbf{E}_G$ , so weight of edge is  $a_{ij} > 0$ , otherwise  $a_{ij} = 0$ . The neighbors set of node  $i$  is  $\mathbf{N}_i = \{(V_j, V_i) \in \mathbf{E}_G\}$ . The degree matrix is defined as  $\mathbf{D} = \text{diag}\{d_1, d_2, \dots, d_N\}$ , where  $d_i = \sum_{j \in \mathbf{N}_i} a_{ij}$ . Laplace matrix is defined as  $\mathbf{L} = \mathbf{D} - \mathbf{A}_G$ . A direct path from node  $i$  to node  $j$  is a sequence of edges  $\{(V_i, V_k), (V_k, V_l), \dots, (V_m, V_j)\}$ . A digraph is said to have a spanning tree, if there is a root node with a direct path from node to every other node in [31].

The  $i$ th secondary-level agent with others realizes the consensus coordinate control of VPS voltage of  $i$ th DG agent with other DGs agents based on digraph  $G_d(\mathbf{V}_G, \mathbf{E}_G, \mathbf{A}_G)$ . Integral consensus is achieved if the VPSs voltages difference between neighbors in digraph as a controller input is transmitted to each consensus controller. Under a distributed coordinate consensus protocol in consensus controller, VPS voltage

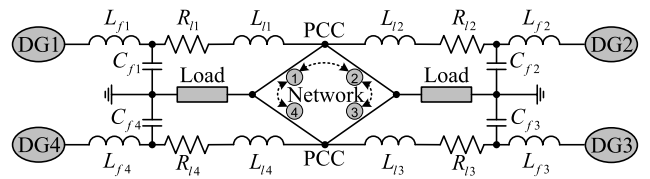


FIGURE 7. Test model with four parallel DGs and several public loads.

dynamic model of  $i$ th DG is described as

$$\dot{x}_i = u_i \tag{14}$$

where  $x_i = [v_{\xi di} \ v_{\xi qi}]^T$  is the state matrix, and  $u_i$  is the control input of  $i$ th consensus controller which is expressed as

$$u_i = cK \sum_{j \in \mathbf{N}_i} a_{ij}(x_i - x_j) \tag{15}$$

where  $a_{ij}$  is the element of adjacency matrix,  $c$  is a positive coupling gain, and  $K > 0$  is a constant.

For a microgrid including  $N$  DGs, the global matrix of state variables is  $\mathbf{x} = [x_1 \ x_2 \ \dots \ x_N]^T$  and global matrix of controller inputs is  $\mathbf{u} = [u_1 \ u_2 \ \dots \ u_N]^T$ , expressed as

$$\mathbf{u} = cK \cdot \mathbf{L}\mathbf{x} \tag{16}$$

*Theorem 1:* Consensus is achieved if there is a spanning tree or a root node with a direct path from node  $i$  to every other node in the digraph. Besides, all the eigenvalues of Laplace matrix  $\mathbf{L}$  have a positive real part except one zero eigenvalue.

*Remarks 1:* The eigenvalues of Laplace matrix  $\mathbf{L}$  are denoted as  $\lambda_i$ . The stability properties of global dynamics in (16) is equivalent to the stability properties of follows

$$\dot{z}_i = -\lambda_i cK z_i \quad i = 1, 2, \dots, N \tag{17}$$

The stability criterion requires  $c$  to be selected as [31]

$$c = \max \left( \frac{1}{2 \min_{i \in N} \text{Re}(\lambda_i)}, 1 \right) \tag{18}$$

The detailed proofs are based on [20].

The amplitude of  $i$ th actual VPS voltage is

$$V_{\xi i} = \sqrt{v_{\xi di}^2 + v_{\xi qi}^2} \tag{19}$$

Synchronization of VPSs voltages as the final goal is realized, gradually maintaining accurate reactive power sharing.

$$\lim_{j \in \mathbf{N}_i} |E_{\xi i} - E_{\xi j}| = 0 \tag{20}$$

$$\lim_{j \in \mathbf{N}_i} |n_{\xi i} Q_i - n_{\xi j} Q_j| = 0 \tag{21}$$

**IV. SIMULATION**

The proposed hierarchical control is verified by a microgrid model in RTLAB and MATLAB/Simulink. As shown in Fig. 7, the test model consists of 4 DGs and several public loads. The transmission lines are modeled as

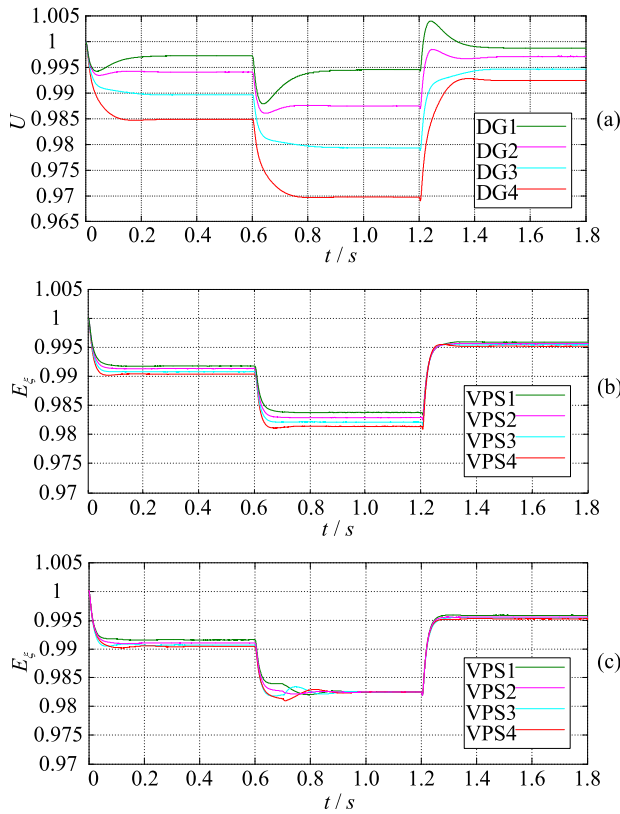


FIGURE 8. DGs voltages magnitudes in case1. (a) traditional method; (b) proposed method without secondary control; (c) proposed method.

TABLE 1. Parameters of the test model

Parameter	Symbol	Value(DG1,DG2,DG3,DG4)
DC link voltage	$U_{dc}$	700V
DG voltage reference	$U^*$	311V
Power reference	$P^*, Q^*$	0W, 0VAr
Droop coefficient	$m_z$	$-4 \times 10^{-5}$
Droop coefficient	$n_z$	$-6 \times 10^{-4}$
Filter inductance	$L_f$	3mH
Filter capacitance	$C_f$	15 $\mu$ F
Filter resistance	$R_f$	0.2 $\Omega$
Line resistance	$R_l$	1.284, 1.124, 0.963, 0.803( $\Omega$ )
Line inductance	$L_l$	0.528, 0.462, 0.396, 0.330(mH)
Virtual resistance	$R_z$	-1.284, -1.124, -0.963, -0.803( $\Omega$ )
Virtual inductance	$L_z$	-0.198, -0.132, -0.066, 0(mH)

RL impedance branches. Simulation parameters are provided in Table 1. The associated adjacency matrix is designed as

$$\mathbf{A}_G = \begin{bmatrix} 0 & 1 & 0 & 1 \\ 1 & 0 & 1 & 0 \\ 0 & 1 & 0 & 0 \\ 1 & 0 & 0 & 0 \end{bmatrix}, \quad \mathbf{D} = \begin{bmatrix} 2 & 0 & 0 & 0 \\ 0 & 2 & 0 & 0 \\ 0 & 0 & 1 & 0 \\ 0 & 0 & 0 & 1 \end{bmatrix},$$

$$\mathbf{L} = \begin{bmatrix} 2 & -1 & 0 & -1 \\ -1 & 2 & -1 & 0 \\ 0 & -1 & 1 & 0 \\ -1 & 0 & 0 & 1 \end{bmatrix} \quad (22)$$

Each DG communicates with each other through the sparse networks. The allowed maximum reactive power deviation is

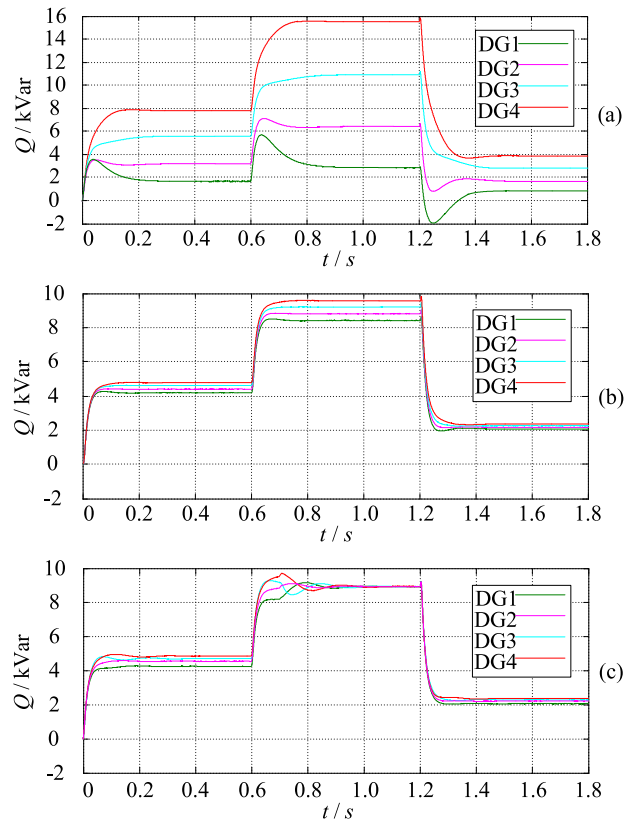
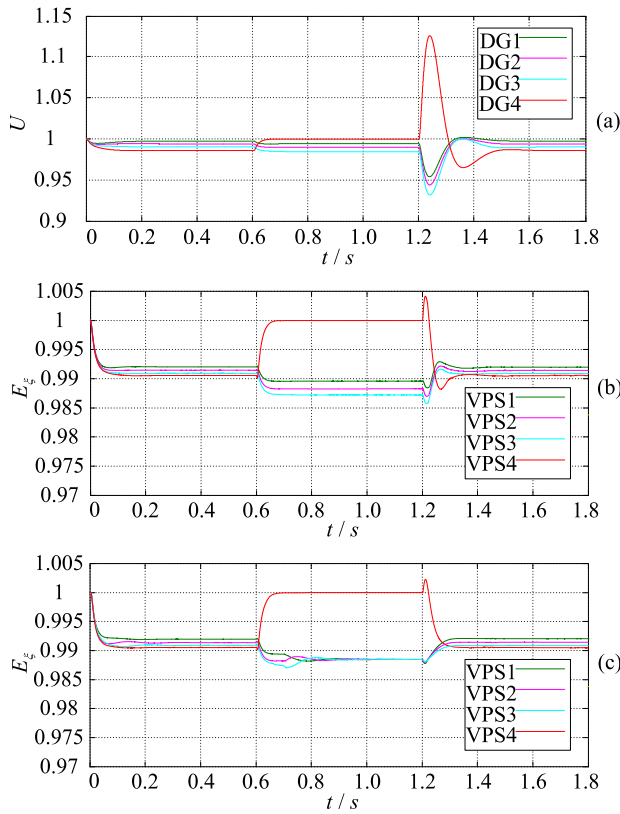


FIGURE 9. Reactive power sharing in case1. (a) traditional method; (b) proposed method without secondary control; (c) proposed method.

$0.5\%Q_{i \max}$  ( $c = 0.5$ ), where  $Q_{i \max}$  are unified to be 100kVar. Voltages of DGs and VPSs are unified as per units based on the bus voltage as reference value. The desired sharing accuracy is  $Q_1 : Q_2 : Q_3 : Q_4 = 1 : 1 : 1 : 1$ . Simulations are conducted in two cases (loads variation; DG plug and play operation).

### A. SIMULATION RESULTS IN CASE1: LOAD VARIATION

Figs. 8-9 show the state performance of DGs voltages amplitudes and reactive powers outputs in case of loads variation. This case, namely case1, is summarized as three stages: increase 18kW+18kVar load powers demands at  $t = 0s$ ; increase 100% load demands at  $t = 0.6s$ ; decrease 150% load demands at  $t = 1.2s$ . As shown in Fig. 8, when load demand increases after  $t = 0s$ , the voltages amplitudes synchronized to nominal voltage amplitude is then lost. Especially in Fig. 8(a), voltage amplitude deviations are relatively large, which is associated with mismatched lines impedance. It directly results in relatively large reactive power sharing inaccuracy in Fig. 9(a), where DG3 and DG4 even run beyond their maximum capacities. In Fig. 8(b), primary control tries to restore all the DGs voltages amplitudes to synchronization, but its effect subjects to small loads power demands. Corresponding to the reactive power sharing in Fig. 9(b), inaccuracies are acceptable in stage1 and stage3,



**FIGURE 10.** DGs voltages magnitudes in case2. (a) traditional method; (b) proposed method without secondary control; (c) proposed method.

but it is unallowable in stage2 for sharing deviation of reactive powers dispatched by DG1 and DG4 is more than 500Var. The secondary control is necessary to normalize the state variables in stage2. As shown in Fig. 8(c), the voltage deviations trigger VVEI at about  $t = 0.7s$  and now the secondary control is activated to synchronize voltages amplitudes, which then restores reactive power sharing accuracy in stage2 of Fig. 9(c). It indicates that primary control cooperating with secondary control guarantee the power sharing accuracy even in the case of relatively large loads power demands. Besides, the coordination role of VVEI is indispensable for controllers switch.

**B. SIMULATION RESULTS IN CASE2: DG PLUG-AND-PLAY OPERATION**

Figs. 10-11 show the state performance of voltage amplitude and reactive power in case of DG plug-and-play operation. This case, namely case2, is also summarized as 3 stages: all DGs plug into network at  $t = 0s$ , DG4 disconnects from network at  $t = 0.6s$ , DG4 plugs into network at  $t = 1.2s$  again. Meanwhile, loads power demands are constant. In Fig. 10, as DGs plug into network at  $t = 0s$ , voltages amplitudes synchronization is also lost. Fig. 10(a) shows voltages amplitudes deviations and poor overshoot performance especially as DG4 plugs into network again. Corresponding to reactive power sharing inaccuracy in Fig. 11(a), where

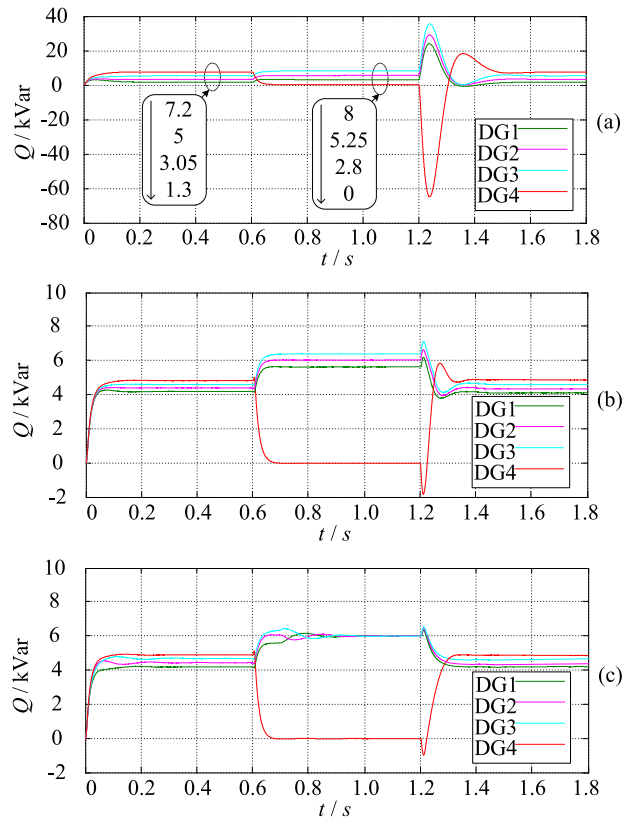


**FIGURE 11.** Reactive power sharing in case2. (a) traditional method; (b) proposed method without secondary control; (c) proposed method.

DG1, DG2 and DG3 even run beyond their maximum capacities and DG4 absorbs reactive power. In Fig. 10(b), voltages synchronization effects of primary control also subject to DG variation which is equivalent to reverse loads variation. Especially in stage2, when DG4 disconnects from network, other DGs start sharing the reactive power part that DG4 should dispatch. Their reactive power sharing inaccuracy in Fig. 11(b) becomes large and unallowable. Overshoot performance in the front of stage3 is improved but still poor. Once applying the secondary control at about  $t = 0.7s$ , strict voltages amplitudes synchronization and accurate power sharing can be realized in Fig. 10(c) and Fig. 11(c). Obviously, the reduced voltage amplitude deviation in stage2 improves the overshoot performance in stage3. Thus, the DG plug-and-play operation is still functional in proposed method.

**V. CONCLUSION**

This paper describes a MAS-based hierarchical distributed coordinate control of VPS in low-voltage microgrid. The DGs interaction manner is based on established MAS. The control system contains two levels controls: distributed primary control can roughly synchronize VPSs voltages by choosing values of virtual impedance, but it is subject to small loads power demands; when loads power demands are relatively big, secondary control based on the consensus theory can



further strictly synchronize VPSs voltages and compensate the above imperfection, and it isn't continuous. VVEI is necessary for coordinating the two levels controls: if one of actual VPSs voltages triggers VVEI, secondary control will activate, otherwise, only primary control participates in synchronous regulation of VPSs voltages. Simulation results coincide with the above theoretical results.

## REFERENCES

- [1] G. A. Pagani and M. Aiello, "Towards decentralization: A topological investigation of the medium and low voltage grid," *IEEE Trans. Smart Grid*, vol. 2, no. 11, pp. 538–547, Sep. 2011.
- [2] S. Anand, B. G. Fernandes, and J. M. Guerrero, "Distributed control to ensure proportional load sharing and improve voltage regulation in low-voltage DC microgrid," *IEEE Trans. Power Electron.*, vol. 28, no. 4, pp. 1900–1913, Apr. 2013.
- [3] J. M. Guerrero, J. C. Vásquez, J. Matas, M. Castilla, and L. G. de Vicuña, "Control strategy for flexible microgrid based on parallel line-interactive UPS systems," *IEEE Trans. Ind. Electron.*, vol. 56, no. 3, pp. 726–736, Mar. 2009.
- [4] M. Kumar, S. C. Srivastava, and S. N. Singh, "Control strategies of a DC microgrid for grid connected and islanded operations," *IEEE Trans. Smart Grid*, vol. 6, no. 4, pp. 1588–1601, Jul. 2015.
- [5] Y. W. Li and C.-N. Kao, "An accurate power control strategy for power-electronics-interfaced distributed generation units operating in a low-voltage multibus microgrid," *IEEE Trans. Power Electron.*, vol. 24, no. 12, pp. 2977–2988, Dec. 2009.
- [6] H. Mahmood, D. Michaelson, and J. Jiang, "Accurate reactive power sharing in an islanded microgrid using adaptive virtual impedances," *IEEE Trans. Power Electron.*, vol. 30, no. 3, pp. 1605–1617, Mar. 2015.
- [7] A. Kahrobaei and Y. A. R. I. Mohamed, "Networked-based hybrid distributed power sharing and control for island microgrid systems," *IEEE Trans. Power Electron.*, vol. 30, no. 2, pp. 603–617, Feb. 2015.
- [8] T. L. Vandoorn, J. D. M. De Kooning, B. Meersman, J. M. Guerrero, and L. Vandevelde, "Automatic power-sharing modification of P/V droop controllers in low-voltage resistive microgrids," *IEEE Trans. Power Del.*, vol. 27, no. 10, pp. 2318–2325, Oct. 2012.
- [9] F. Guo, C. Wen, J. Mao, and Y. D. Song, "Distributed secondary voltage and frequency restoration control of droop-controlled inverter-based microgrids," *IEEE Trans. Ind. Electron.*, vol. 62, no. 7, pp. 4355–4364, Jul. 2015.
- [10] M. Savaghebi, A. Jalilian, J. C. Vásquez, and J. M. Guerrero, "Secondary control scheme for voltage unbalance compensation in an islanded droop-controlled microgrid," *IEEE Trans. Smart Grid*, vol. 3, no. 2, pp. 797–807, Jun. 2012.
- [11] C. Dou, M. Lv, T. Zhao, Y. Ji, and H. Li, "Decentralised coordinate control of microgrid based on multi-agent system," *IET Gener., Transm. Distrib.*, vol. 9, no. 12, pp. 2474–2484, Dec. 2015.
- [12] Y. S. F. Eddy, H. B. Gooi, and S. X. Chen, "Multi-agent system for distributed management of microgrids," *IEEE Trans. Power Syst.*, vol. 30, no. 1, pp. 24–34, Jan. 2015.
- [13] H. Liang, B. J. Choi, W. Zhuang, X. Shen, A. S. A. Awad, and A. Abdr, "Multiagent coordination in microgrids via wireless networks," *IEEE Trans. Wireless Commun.*, vol. 19, no. 6, pp. 1284–1536, Jun. 2012.
- [14] C. Dou, N. Li, D. Yue, and T. Liu, "Hierarchical hybrid control strategy for micro-grid switching stabilisation during operation mode conversion," *IET Gener. Transm. Distrib.*, vol. 10, no. 9, pp. 2880–2890, Sep. 2016.
- [15] A. Bidram, A. Dacoudi, F. L. Lewis, and Z. Qu, "Secondary control of microgrids based on distributed cooperative control of multi-agent system," *IET Gener., Transm. Distrib.*, vol. 7, no. 8, pp. 822–831, Aug. 2013.
- [16] D. Wu, F. Tang, T. Dragicevic, J. C. Vasquez, and J. M. Guerrero, "Autonomous active power control for islanded AC microgrids with photovoltaic generation and energy storage system," *IEEE Trans. Energy Convers.*, vol. 29, no. 4, pp. 882–892, Dec. 2014.
- [17] J. Xiao, P. Wang, L. Setyawan, and Q. Xu, "Multi-level management system for real-time scheduling of dc microgrids with multiple slack terminals," *IEEE Trans. Energy Convers.*, vol. 31, no. 3, pp. 392–400, Mar. 2016.
- [18] D. Shi, R. Sharma, and Y. Ye, "Adaptive control of energy storage for voltage regulation in distribution system," in *Proc. IEEE Int. Conf. Smart Energy Grid Eng.*, Oshawa, ON, Canada, Aug. 2013, pp. 1–7.
- [19] J. He and Y. W. Li, "An enhanced microgrid load demand sharing strategy," *IEEE Trans. Power Electron.*, vol. 27, no. 9, pp. 3984–3995, Sep. 2012.
- [20] A. Bidram, A. Davoudi, F. L. Lewis, and J. M. Guerrero, "Distributed cooperative secondary control of microgrids using feedback linearization," *IEEE Trans. Power Syst.*, vol. 28, no. 3, pp. 3462–3470, Aug. 2013.
- [21] Y. Xu, "Optimal distributed charging rate control of plug-in electric vehicles for demand management," *IEEE Trans. Power Syst.*, vol. 30, no. 5, pp. 1536–1545, May 2015.
- [22] L. Meng et al., "Distributed voltage unbalance compensation in islanded microgrids by using a dynamic consensus algorithm," *IEEE Trans. Power Electron.*, vol. 31, no. 1, pp. 827–838, Jan. 2016.
- [23] C. Huang and X. Ye, "A nonlinear transformation for reaching dynamic consensus in multi-agent systems," *IEEE Trans. Autom. Control.*, vol. 60, no. 12, pp. 3263–3268, Dec. 2015.
- [24] Z. Li, Z. Duan, and G. Chen, "Dynamic consensus of linear multi-agent systems," *IET Control Theory Appl.*, vol. 5, no. 1, pp. 19–28, Jan. 2011.
- [25] J. Yu, C. Dou, and X. Li, "MAS-based energy management strategies for a hybrid energy generation system," *IEEE Trans. Ind. Electron.*, vol. 63, no. 6, pp. 3756–3764, Jun. 2016.
- [26] C. X. Dou and B. Liu, "Multi-agent based hierarchical hybrid control for smart microgrid," *IEEE Trans. Smart Grid*, vol. 4, no. 2, pp. 771–778, Jun. 2013.
- [27] X. Wang, F. Blaabjerg, and Z. Chen, "Autonomous control of inverter-interfaced distributed generation units for harmonic current filtering and resonance damping in an islanded microgrid," *IEEE Trans. Ind. Appl.*, vol. 50, no. 2, pp. 452–461, Jan./Feb. 2014.
- [28] B. K. Sahu, S. Pati, and S. Panda, "Hybrid differential evolution particle swarm optimisation optimised fuzzy proportional-integral derivative controller for automatic generation control of interconnected power system," *IET Gener. Transm. Distrib.*, vol. 8, no. 11, pp. 1789–1800, Nov. 2014.
- [29] L. Meng, T. Dragicevic, J. R. Perez, J. C. Vasquez, and J. M. Guerrero, "Modeling and sensitivity study of consensus algorithm-based distributed hierarchical control for DC microgrids," *IEEE Trans. Smart Grid*, vol. 7, no. 5, pp. 1504–1515, May 2016.
- [30] C. Dou, D. Yue, X. Li, and Y. Xue, "MAS-based management and control strategies for integrated hybrid energy system," *IEEE Trans. Ind. Informat.*, vol. 12, no. 8, pp. 1332–1349, Aug. 2016.
- [31] L. Y. Lu and C. C. Chu, "Consensus-based droop control synthesis for multiple DICs in isolated micro-grids," *IEEE Trans. Power Syst.*, vol. 30, no. 5, pp. 2243–2256, Sep. 2015.



**CHUNXIA DOU** received the B.S. and M.S. degrees in automation from the Northeast Heavy Machinery Institute, Qiqihaer, China, in 1989 and 1994, respectively, and the Ph.D. degree from the Institute of Electrical Engineering, Yanshan University, Qinhuangdao, China, in 2005. In 2010, she joined the Department of Engineering, Peking University, Beijing, China, where she was a Post-doctoral Fellow for two years. Since 2005, she has been a Professor with the Institute of Electrical Engineering, Yanshan University. Her current research interests include multi-agent-based control, event-triggered hybrid control, distributed coordinated control, and multi-mode switching control, and their applications in power systems, microgrids, and smart grids.

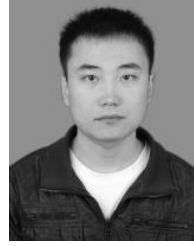


**ZHANQIANG ZHANG** received the dual B.S. degree in electrical engineering and automation/mathematics and applied mathematics from Hebei University of Science and Technology, Shijiazhuang, China, in 2015. He is currently pursuing the M.S. degree in automation at Yanshan University, Qinhuangdao, China. His current research interests include microgrids power coordinate control and distributed generation technology.



**DONG YUE** (SM'08) received the Ph.D. degree from the South China University of Technology, Guangzhou, China, in 1995. He is currently a Professor and the Dean of the Institute of Advanced Technology, Nanjing University of Posts and Telecommunications, and also a Changjiang Professor with the Department of Control Science and Engineering, Huazhong University of Science and Technology. He has authored over 100 papers published in international journals, domestic journals,

and international conference proceedings. His current research interests include analysis and synthesis of networked control systems, multi-agent systems, optimal control of power systems, and internet of things. He is currently an Associate Editor of the IEEE Control Systems Society Conference Editorial Board and also an Associate Editor of the IEEE TRANSACTIONS ON NEURAL NETWORKS AND LEARNING SYSTEMS, *Journal of the Franklin Institute* and *International Journal of Systems Science*.



**YUHANG ZHENG** received the B.S. degree in automation from Liren College, Yanshan University, Qinhuangdao, China, in 2015. He is currently pursuing the M.S. degree in pattern recognition and intelligent systems at Yanshan University. His current research interests include renewable energy forecasting control and energy management systems analysis in microgrids.

...